Electronic Supplementary Material (ESI) for ChemComm.

Supplementary Information

Reversible pH-responsive MRI contrast with paramagnetic polymer micelles

Connor M. Ellis,[a] Daohe Yuan,[a] Ferenc Mózes,[b] Jack Miller[b,c,d] and Jason J. Davis*[a]

a. Department of Chemistry, University of Oxford, South Parks Road, Oxford, OX1 3QZ, UK
b. Oxford Center for Clinical Magnetic Resonance Research, Radcliffe Department of Medicine, University of Oxford, Level 0, John Radcliffe Hospital, Oxford, OX3 9DU, UK
c. The MR Research Centre, Aarhus University, Aarhus 8200, Denmark
d. Department of Physics, Clarendon Laboratory, Parks Road, Oxford, OX1 3PU, UK

E-mail: jason.davis@chem.ox.ac.uk; Fax: +44 (0)1865 272 690; Tel: +44 (0)1865 275 914

Experimental Section

Chemicals:

N,N-dimethylformamide (DMF) and diethyl ether (Et_2O) were purchased from Thermo Fisher Scientific. All other chemicals were purchased from Merck and used as received unless otherwise stated. Ultrapure water (Millipore) with a resistivity of 18.2 MΩ·cm was used throughout.

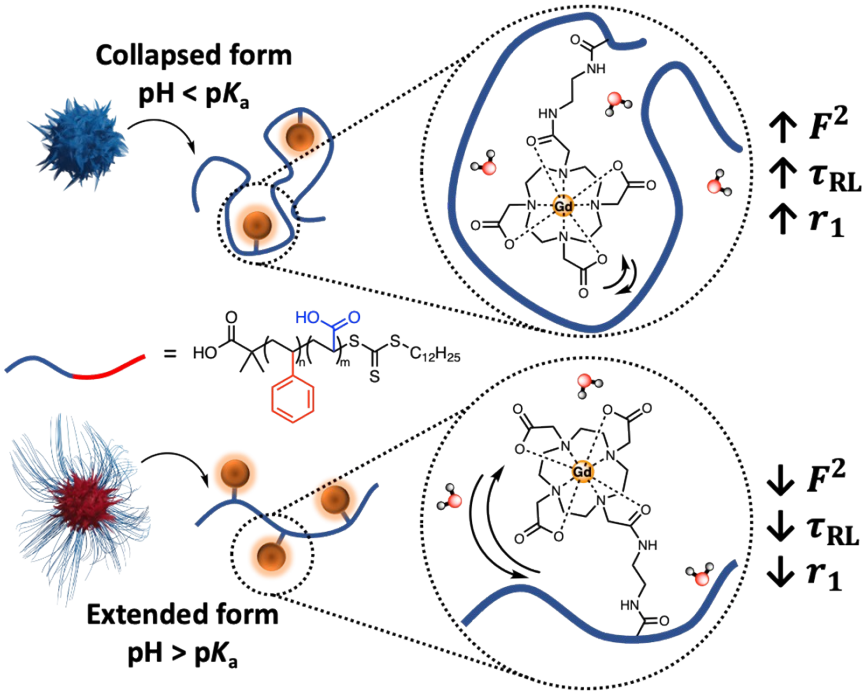

ESI 1. A schematic highlighting how changes in pH affect the conformation of PAA and, by extension, the observed relaxivity of the micellular contrast agent. This is facilitated through differences in chelate rotational correlation times (τ_{RL}), with strong core coupling ($F^2 \rightarrow 1$) at low pH responsible for enhanced r_1.

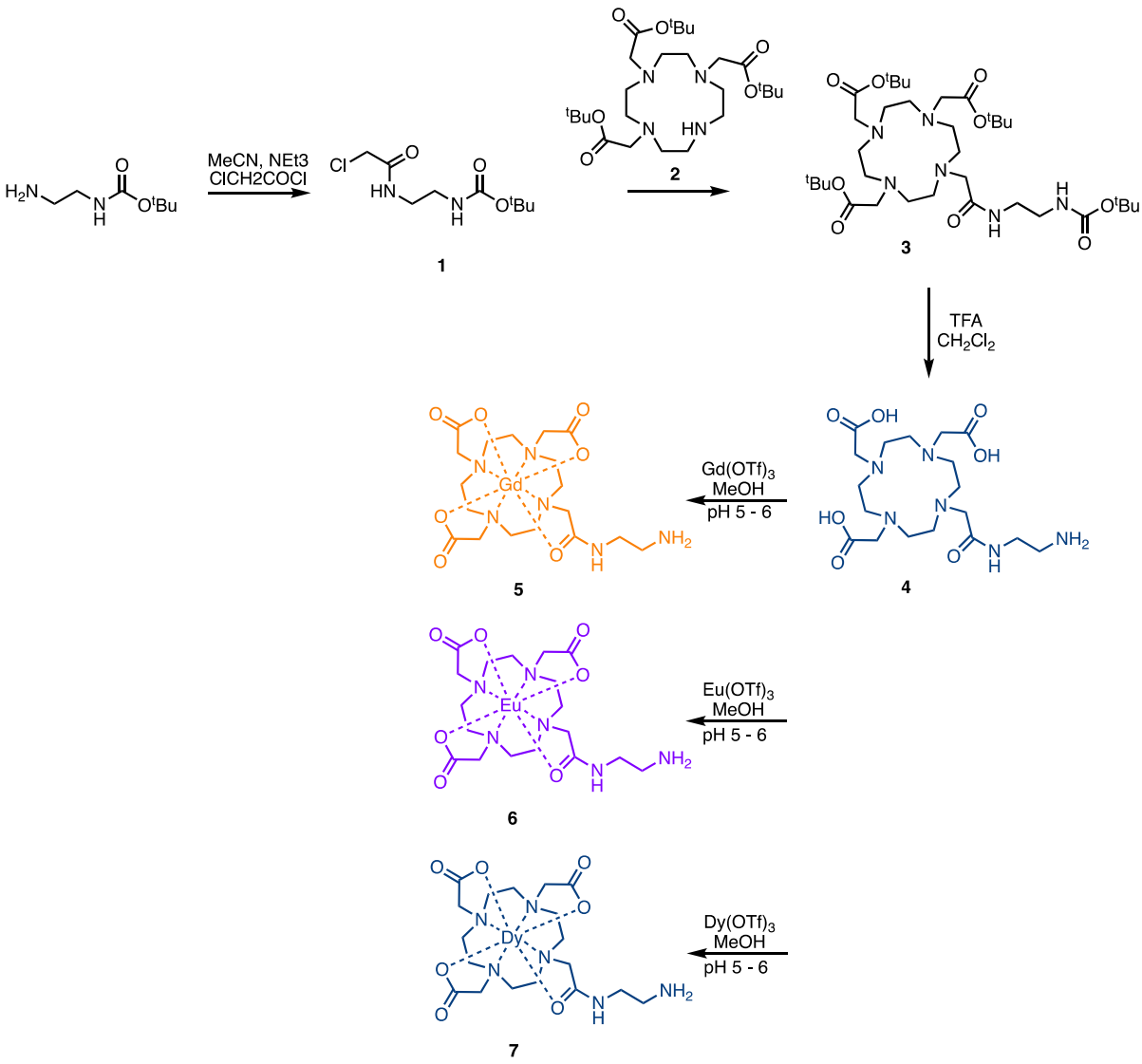

ESI 2. Reaction scheme for the synthesis of the Ln-DO3A ligands used in this work with an amine pendant arm to facilitate molecular tethering to the polymer.

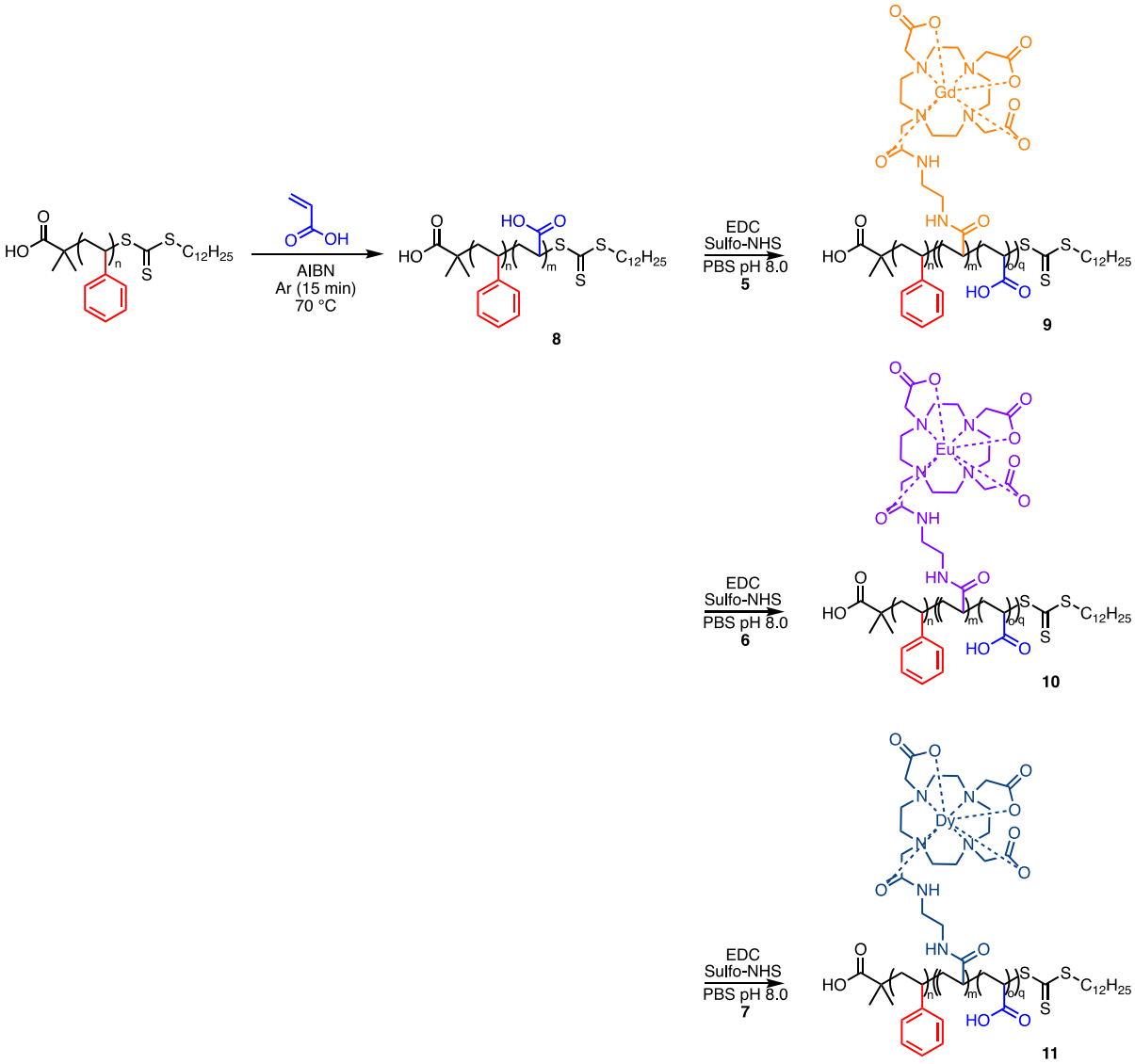

ESI 3. Reaction scheme summarising the synthesis of the PAA-*b*-PS polymers and the subsequent tethering of the desired Ln-DO3A ligand.

The synthesis of compounds **1 – 6** was achieved by the use of a modified literature procedure.[1]

_N_-(_tert_-butoxycarbonyl)-_N'_-aminoacetylchloride (1)

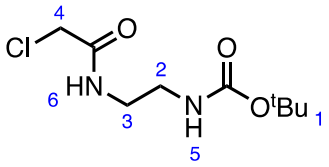

_N_-(_tert_-butoxycarbonyl)-1,2-diaminoethane (1 g, 6.25 mmol) and Et_3N (2 mL) were dissolved in MeCN (20 mL), with chloroacetylchloride added drop-wise over a period of 30 min to the solution under stirring. The solution was then left to stir for 24 h at r.t. (reaction progress monitored by TLC), after which the solvents were removed under reduced pressure. The solid was then dissolved in CH_2Cl_2 and washed with H_2O. The product was recrystallised from EtOAc/hexane to yield a white precipitate that was collected and air dried. ***^{1}H NMR*** *(400 MHz, $CDCl_3$) δ_H = 1.45 (9H, s, tert-butyl CH_3, H^1), 3.33 (2H, m, bocNCH_2, H^2), 3.41 (2H, m, CH_2, H^3), 4.04 (2H, m, COCH_2Cl, H^4), 4.86 (1H, bs, bocNH, H^5), 7.18 (1H, bs, NH, H^6).*

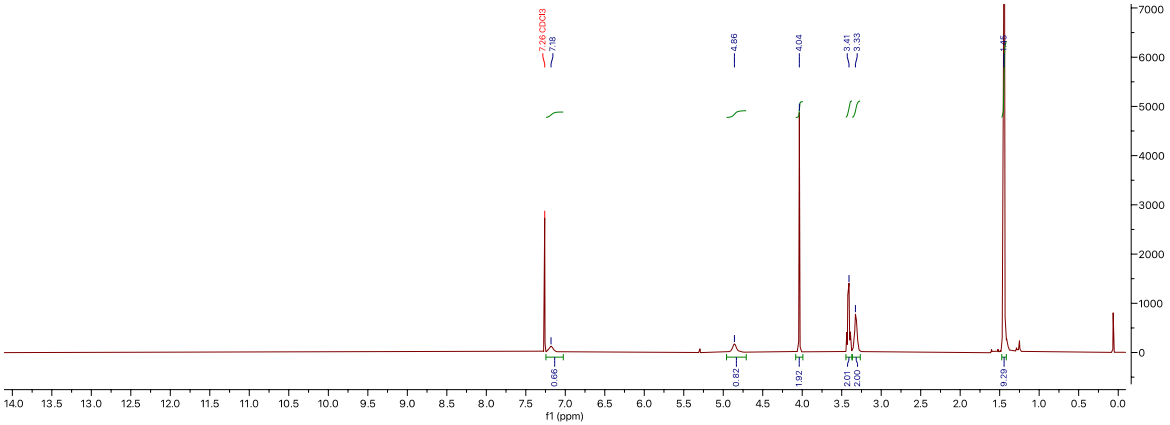

ESI 4. NMR spectrum for N-(tert-butoxycarbonyl)-N'-aminoacetylchloride.

1,4,7-tris(*tert*-butoxycarbonylmethyl)-1,4,7,10-tetraazacyclododecane, hydrobromide salt (2)

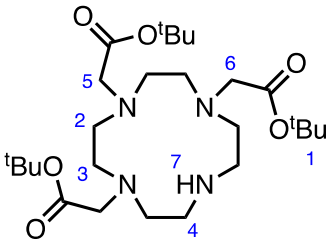

1,4,7,10-tetraazacyclododecane (cyclen, 2.5 g, 0.015 mol) was dissolved in MeCN (84.2 mL), with $NaHCO_3$ (4.023 g) subsequently added to the solution. The mixture was cooled to 0 °C with *t*-butyl bromoacetate (16.97 mL) then added dropwise (1 mL/min). The reaction was then left for 2 days at room temperature (r.t.). The inorganic salt was removed by filtration, with the filtrate concentrated by rotary evaporation. The crude product was re-suspended in 50 mL toluene and heated. Any large solid product was broken down to fine pieces using a spatula/sonication. Any insoluble product was filtered off and washed twice more with toluene to fully obtain the desired product. ***^{1}H NMR*** *(400 MHz, $CDCl_3$) δ_H = 1.46 (27H, 2 x s, tert-butyl CH_3, H^1), 2.88 (4H, bs, NCH_2, H^2), 2.92 (8H, bs, NCH_2, H^3), 3.10 (4H, bs, CH_2, H^4), 3.29 (2H, s, $COCH_2N$, H^5), 3.37 (4H, s, $COCH_2N$, H^6), 10.08 (1H, NH, H^7).*

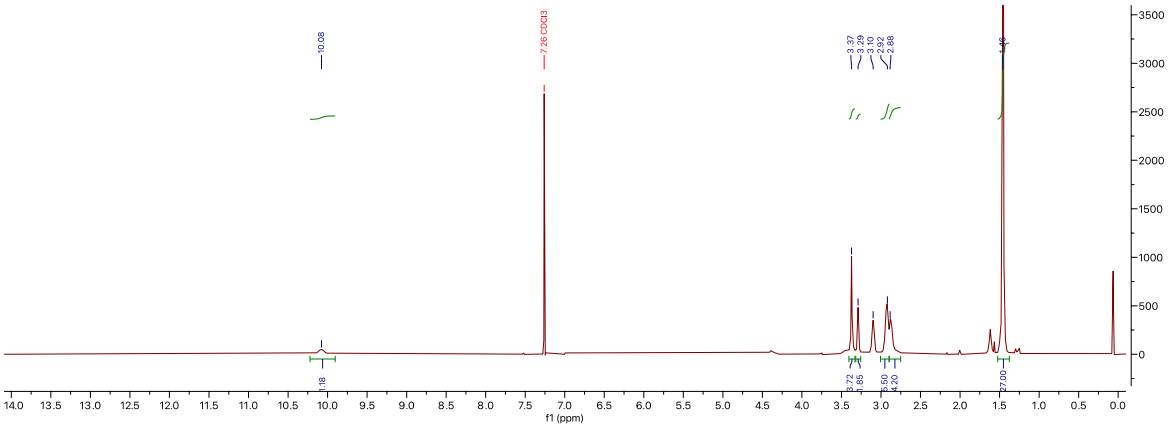

ESI 5. NMR spectrum for 1,4,7-tris(tert-butoxycarbonylmethyl)-1,4,7,10-tetraazacyclododecane, hydrobromide salt.

1,4,7-tris(*tert*-butoxycarbonylmethyl)-10-(*N*-(2-*tert*-butoxycarbonylaminoethyl)acetamide)-1,4,7,10-tetraazacyclododecane (3)

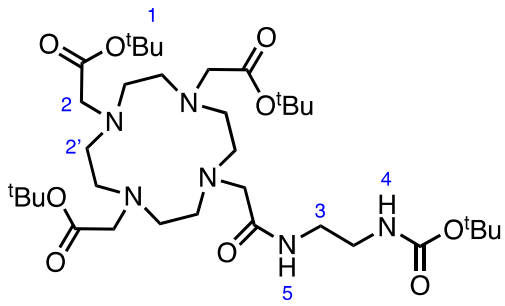

2 (1.00 g, 1.68 mmol), **1** (0.40 g, 1.68 mmol) and $NaHCO_3$ (1.00 g, 12 mmol) were dissolved in MeCN (10 mL) and heated under reflux for 24 h. The solution was then filtered and evaporated to dryness. The compound was purified by column chromatography on silica (CH_2Cl_2/MeOH, 99:1), with the main yellow band collected and evaporated to dryness to yield a yellow solid. *800 mg, 67 %.* ***^{1}H NMR*** *(400 MHz, $CDCl_3$) δ_H = 1.41 (36H, s, tert-Bu, H^1), 2.33 (24H, br (not resolved), CH_2, H^2, $H^{2'}$), 3.29 (4H, s, $NHCH_2CH_2NH$, H^3), 5.93 (1H, s, NHboc, H^4), 8.54 (1H, s, CONH, H^5).* ***ES$^+$ MS*** *(1:1 H_2O:MeCN) m/z = 714.49, found: 714.79 $\{M\}^+$.*

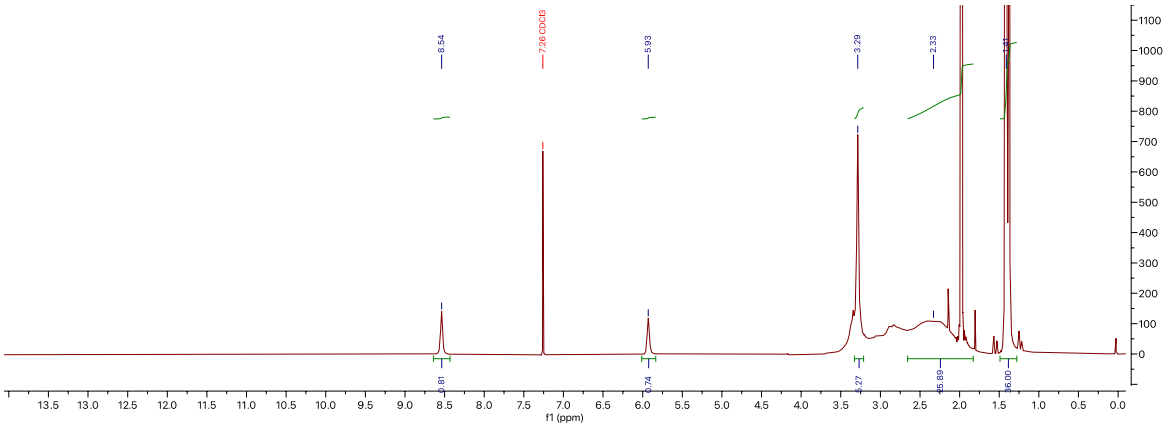

ESI 6. NMR spectrum for 1,4,7-Tris(tert-butoxycarbonylmethyl)-10-(N-(2-tert-butoxycarbonylaminoethyl)acetamide)-1,4,7,10-tetraazacyclododecane.

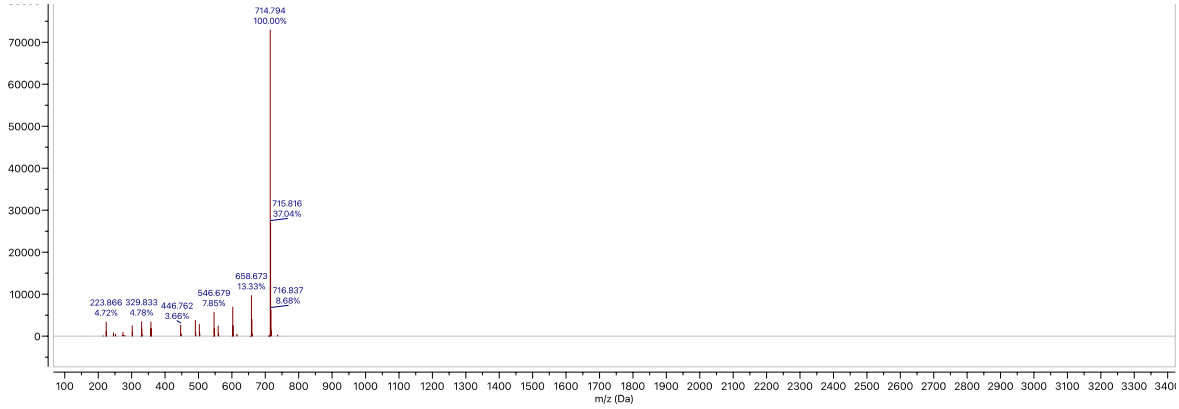

ESI 7. Mass spectrum for 1,4,7-Tris(tert-butoxycarbonylmethyl)-10-(N-(2-tert-butoxycarbonylaminoethyl)acetamide)-1,4,7,10-tetraazacyclododecane.

1,4,7-Tris(carbonylmethyl)-10-(aminoethyl-*N'*-acetyl)-1,4,7,10-tetraazacyclododecane (4)

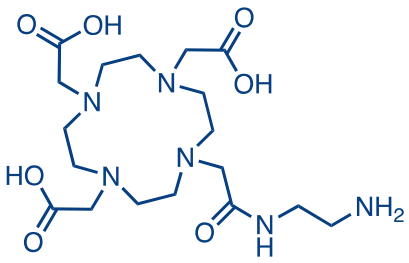

3 (800 mg, 1.03 mmol) was dissolved in CH_2Cl_2 (10 mL), with TFA then added dropwise (5 mL) and the solution stirred for 24 h. The solvent was removed under reduced pressure and the residue was purified by dissolving in the minimum amount of MeOH and precipitating out in Et_2O. This was repeated for a total of three times and left to dry under vacuum overnight to afford an off-white solid. *425 mg, 92 %.* ***^{1}H NMR*** *(400 MHz, $CDCl_3$) δ_H = 3.0 – 3.60 (28H, br (not resolved), all CH_2's).* ***ES$^+$ MS*** *(1:1 H_2O:MeCN) m/z = 446.25, found: 446.72 $\{M+H\}^+$.*

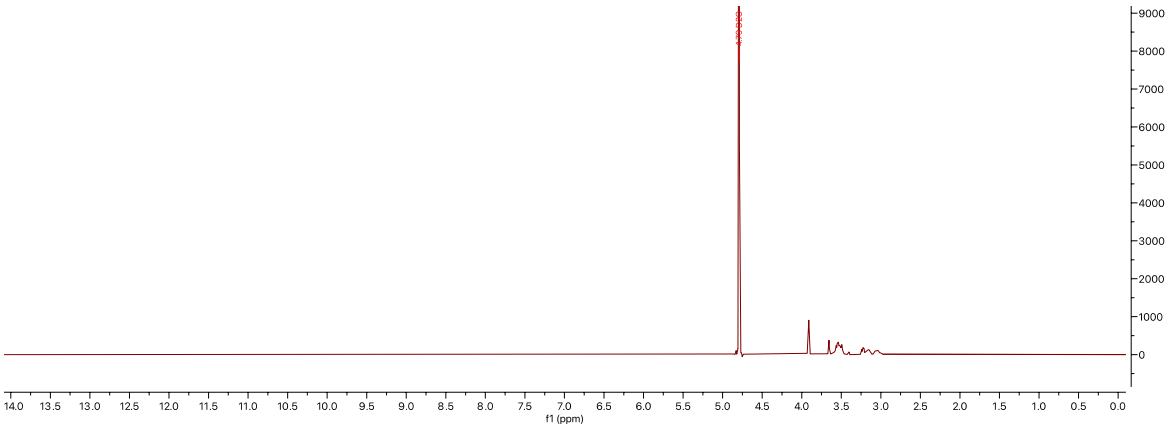

ESI 8. Full NMR spectrum for 1,4,7-Tris(carbonylmethyl)-10-(aminoethyl-N'-acetyl)-1,4,7,10-tetraazacyclododecane.

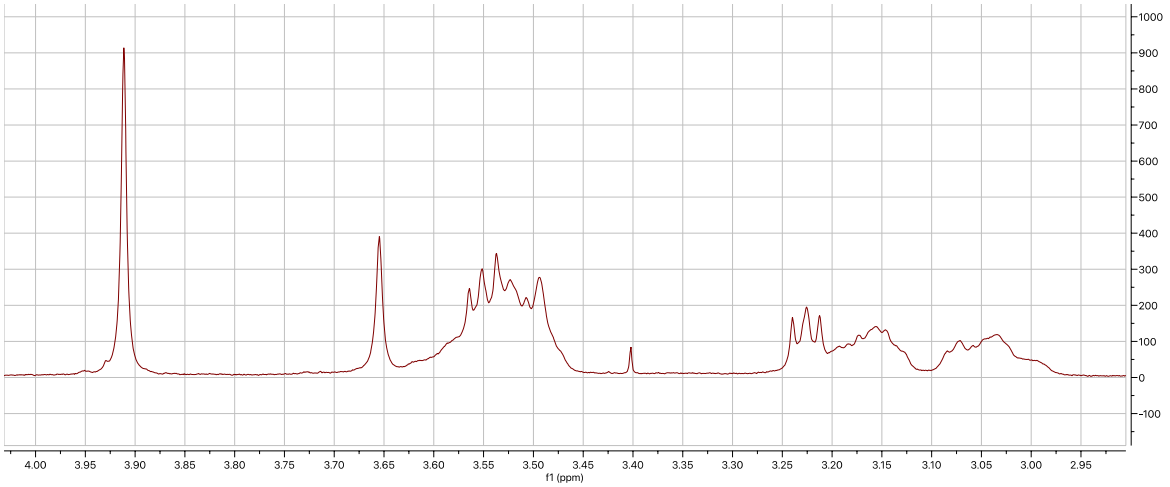

ESI 9. Magnified NMR spectrum for 1,4,7-Tris(carbonylmethyl)-10-(aminoethyl-N'-acetyl)-1,4,7,10-tetraazacyclododecane.

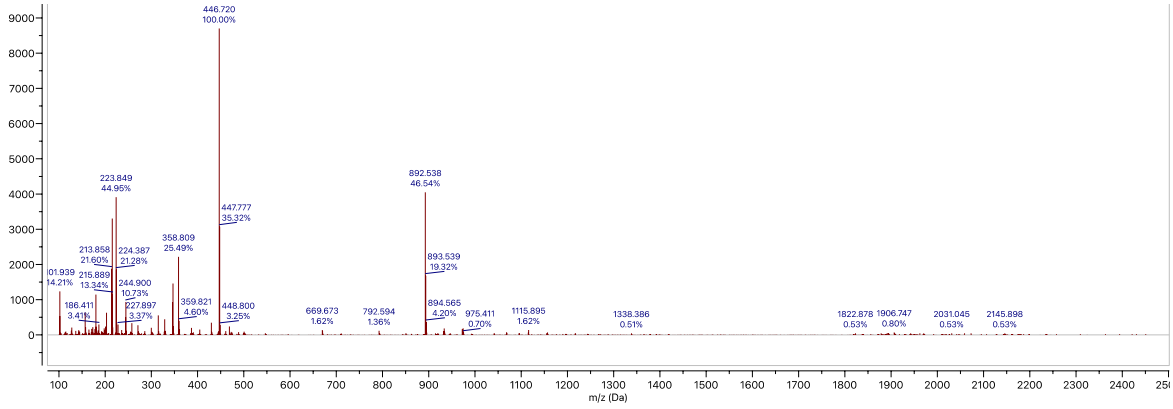

ESI 10. Mass spectrum for 1,4,7-Tris(carbonylmethyl)-10-(aminoethyl-*N'*-acetyl)-1,4,7,10-tetraazacyclododecane.

Gadolinium(III)-1,4,7-Tris(carbonylmethyl)-10-(aminoethyl-*N'*-acetyl)-1,4,7,10-tetraazacyclododecane (5)

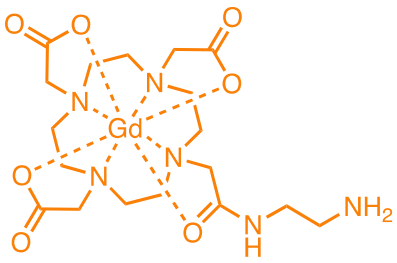

4 (66.5 mg, 0.118 mmol) was dissolved in MeOH (3 mL) to which 0.13 mmol $Gd(OTf)_3$ (78.6 mg) was added. The mixture was left stirring at 65 °C for 1 h, after which the pH was adjusted to pH 5.0 using sodium hydroxide (NaOH, 1 M). The reaction was then left stirring at 65 °C for a further 23 h. The solvent was removed under reduced pressure to afford the solid product. The solid product was dissolved in 3 mL H_2O, after which NaOH (1 M) was added to adjust the pH (pH 9.0/10.0), to precipitate out any remaining $Gd(OTf)_3$ salts. These were removed by centrifugation (7000 rpm, 10 min), with the supernatant collected (containing the desired product) and neutralised to pH 6.0/7.0 using hydrochloric acid (1 M, HCl). The solvent was removed under N_2 to yield the purified product. ***ES*$^+$ *MS*** *(1:1 H_2O:MeCN) m/z = 601.15, found: 619.79.*

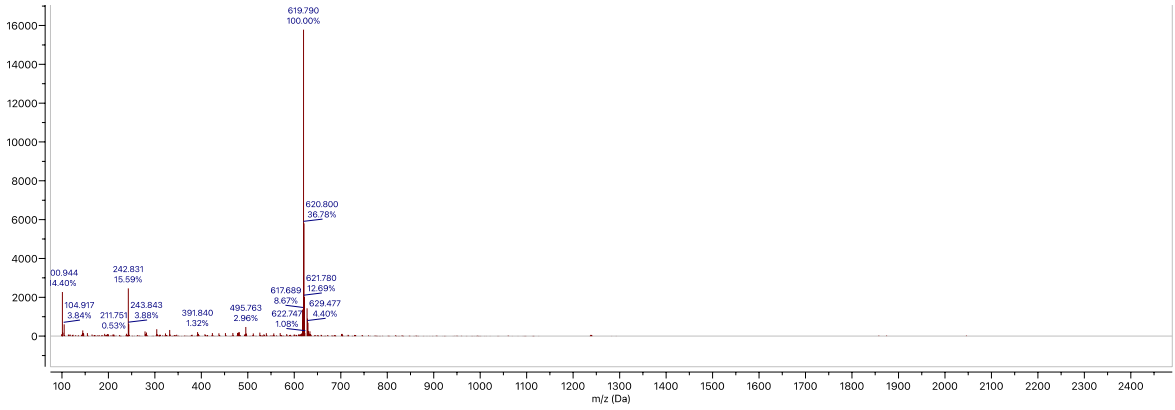

ESI 11. Mass spectrum for gadolinium(III)-1,4,7-Tris(carbonylmethyl)-10-(aminoethyl-N'-acetyl)-1,4,7,10-tetraazacyclododecane.

Europium(III)-1,4,7-Tris(carbonylmethyl)-10-(aminoethyl-*N'*-acetyl)-1,4,7,10-tetraazacyclododecane (6)

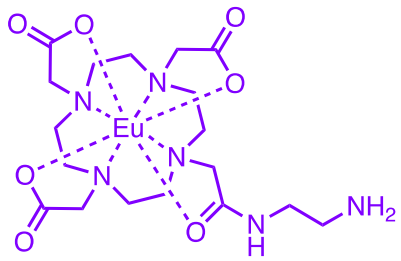

4 (66.5 mg, 0.118 mmol) was dissolved in MeOH (3 mL) to which 0.13 mmol $Eu(OTf)_3$ (77.4 mg) was added. The reaction was stirred at 65 °C for 1 h. The pH was then adjusted to pH 5.0/6.0 using 1 M NaOH and checking with indicator paper, with the reaction stirred for a further 23 h. The solvent was then removed under reduced pressure. The complex was dissolved in 3 mL H_2O, with the pH of the resulting solution adjusted to pH 9.0/10.0 (to precipitate out any remaining $Eu(OTf)_3$ salts) using 1 M NaOH. This was then centrifuged at 7000 rpm for 10 min, with the supernant collected (containing the desired product) and neutralised to pH 6.0/7.0 using 1 M HCl. The solvent was removed under a stream of N_2 to afford the desired solid product. ***^{1}H NMR*** *(400 MHz, D_2O) δ33.78 (s), 31.68 (s), 30.57 (s), 12.23 (s), 10.98 (s), 10.36 (s), -11.03 (s), -11.40 (s), -12.60 (s), -13.70 (s), -14.03 (s), -15.01 (s), -15.68 (s), -16.79 (s). Only resolved peaks outside the 10 to -10 ppm range are reported.* ***ES$^+$ MS*** *(1:1 H_2O:MeCN) m/z = 596.15, found: 597.1 {M+H}$^+$.*

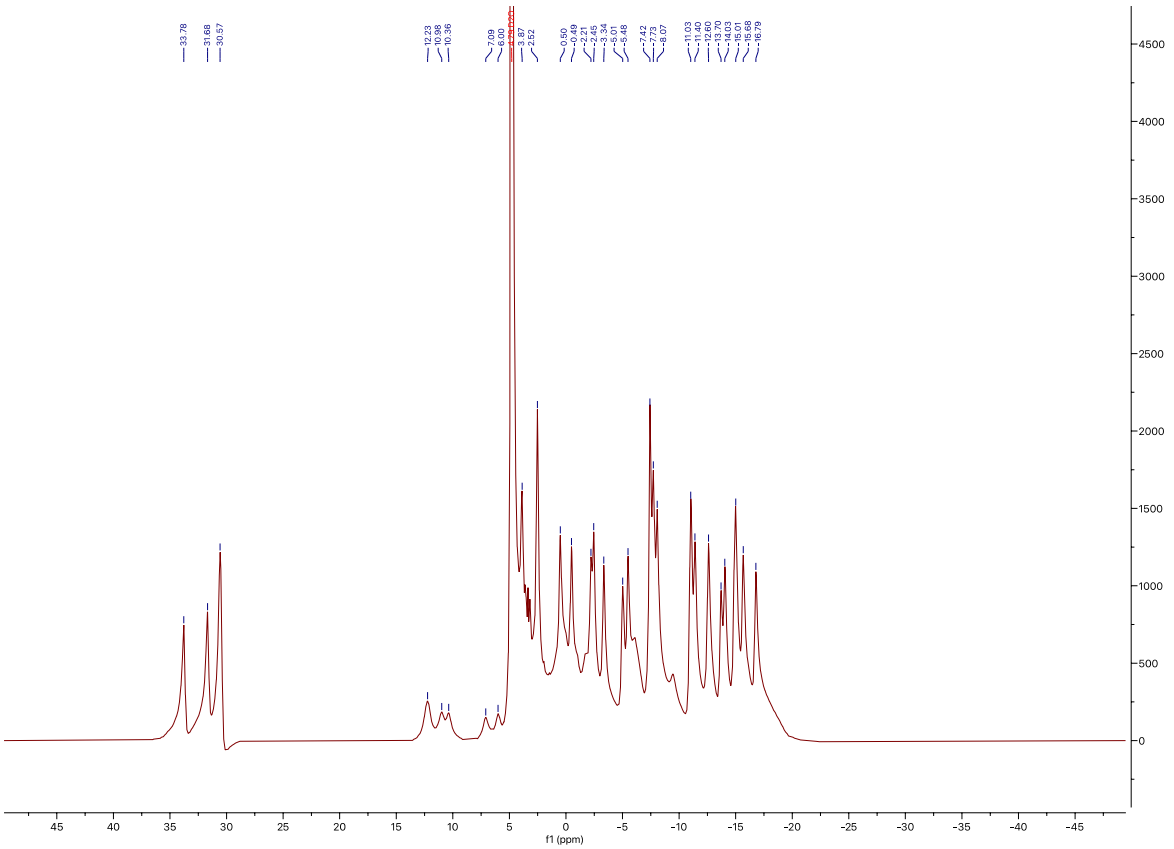

ESI 12. NMR spectrum for europium(III)-1,4,7-Tris(carbonylmethyl)-10-(aminoethyl-N'-acetyl)-1,4,7,10-tetraazacyclododecane.

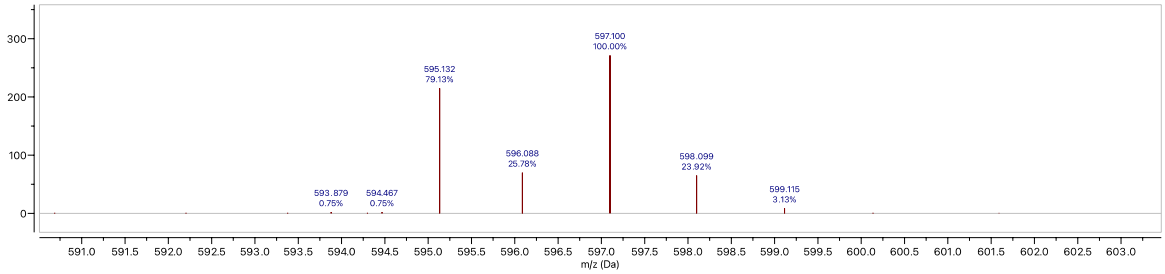

ESI 13. Mass spectrum for europium(III)-1,4,7-Tris(carbonylmethyl)-10-(aminoethyl-N'-acetyl)-1,4,7,10-tetraazacyclododecane

Dysprosium(III)-1,4,7-Tris(carbonylmethyl)-10-(aminoethyl-*N*'-acetyl)-1,4,7,10-tetraazacyclododecane (7)

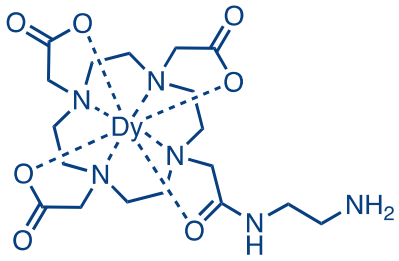

4 (66.5 mg, 0.118 mmol) was dissolved in MeOH (3 mL) to which 0.13 mmol $Dy(OTf)_3$ (79.3 mg) was added. The mixture was left stirring at 65 °C for 1 h, after which the pH was adjusted to pH 5.0 using sodium hydroxide (NaOH, 1 M). The reaction was then left stirring at 65 °C for a further 23 h. The solvent was removed under reduced pressure to afford the solid product. The solid product was dissolved in 3 mL H_2O, after which NaOH (1 M) was added to adjust the pH (pH 9.0/10.0), to precipitate out any remaining $Dy(OTf)_3$ salts. These were removed by centrifugation (7000 rpm, 10 min), with the supernatant collected (containing the desired product) and neutralised to pH 6.0/7.0 using hydrochloric acid (1 M, HCl). The solvent was removed under N_2 to yield the purified product. ***ES*$^+$ *MS*** *(1:1 H_2O:MeCN) m/z = 607.15, found: 606.29.*

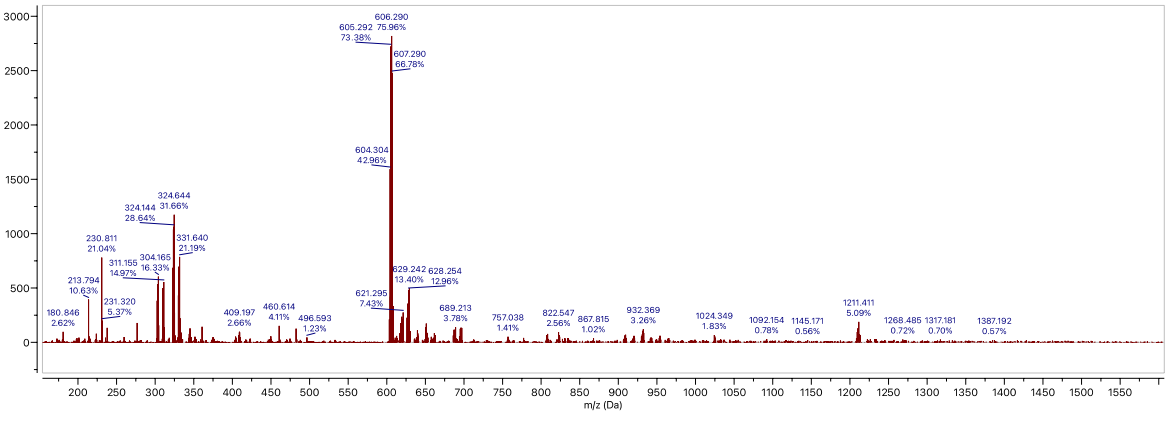

ESI 14. Mass spectrum for dysprosium(III)-1,4,7-Tris(carbonylmethyl)-10-(aminoethyl-N'-acetyl)-1,4,7,10-tetraazacyclododecane.

Poly(styrene)-*block*-poly(acrylic acid) (PS-*b*-PAA) (8)

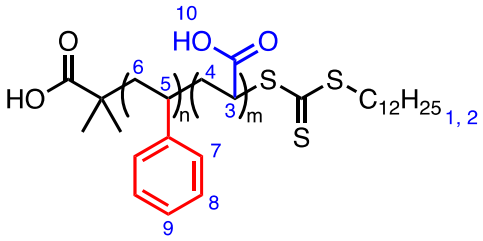

Polystyrene (2-(dodecylthiocarbonothioylthio)-2-methylpropanoic acid (DDMAT) terminated) (25 mg, 5 μmol), acrylic acid (AA, 0.0686 mL, 1 mmol) and azobisisobutyronitrile (AIBN, 0.1642 mg, 1 μmol) were added to a Biotage® microwave reaction vial and dissolved in dimethylformamide (DMF) to a total volume of 1 mL. The solution was degassed in argon for 15 mins before stirring at 70 °C for 18 h. The reaction was purified by centrifugation where a small volume of DMF was used to redissolve the polymer, which was then reprecipitated out by adding diethyl ether, with the process repeated for a total of three times (with the resulting product denoted PS-*b*-PAA). ***¹H NMR*** *(400 MHz, DMSO) δ0.86 (3 H, terminal -CH_3 of -$C_{12}H_{25}$, H^1), 1.23 (22 H, –$CH_2(CH_2)_{10}CH_3$ of alkyl chain, H^2), 1.51 – 2.21 (–CH and –CH_2 of PAA and PS backbone, H^3 – H^6), 6.56 and 7.06 (5 H, –Ph–H of PS block, H^7 – H^9) and 12.20 (–COOH of PAA block, H^{10}).*

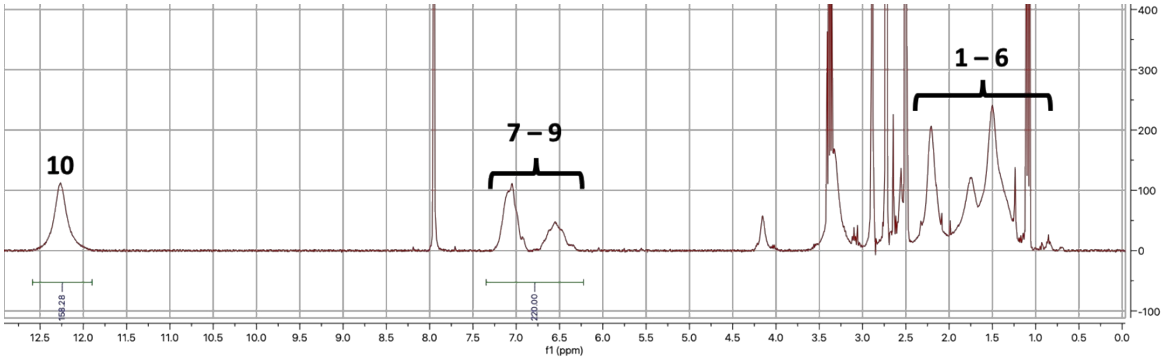

ESI 15. NMR spectrum for the PAA-*b*-PS block copolymer with the key peaks highlighted.

Paramagnetically-doped micelles: Gd-PAA-*b*-PS (9)

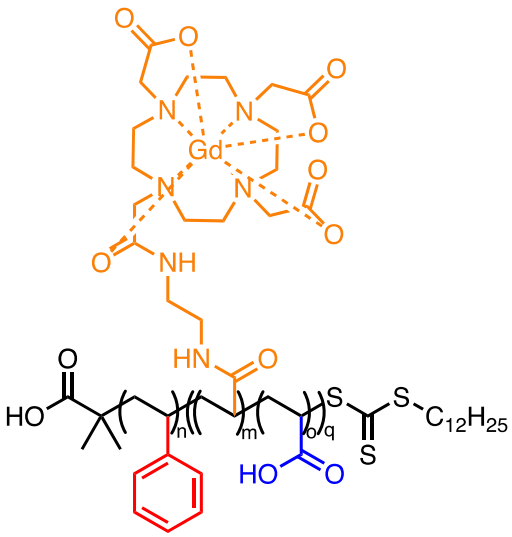

PS-*b*-PAA (**8**, 40 mg) was dispersed in H_2O (7 mL), and the reaction adjusted to pH = 8.0 using NaOH (1 M), with 1-ethyl-3-(3-dimethylaminopropyl)carbodiimide (EDC, 24 mg, 0.155 mmol) and *N*-hydroxysulfosuccinimide sodium salt (sulfo-NHS, 30 mg, 0.138 mmol) then added to the reaction flask. After 30 min, 5.0 mg of **5** dissolved in of PBS (2 mL, pH = 8.0) was added. The reaction underwent vigorous stirring at r.t for 24 h. The solvent was removed under a stream of N_2 to afford the crude product. Afterwards, the resulting polymers were collected by washing with water three times, collecting the supernant (contains the dissolved polymer), and vacuuming off. This ensures the complete removal of any unreacted PS. Then the polymers were washed two times in MeOH to remove any unreacted reagents and left to dry under vacuum.

Optically active micelles: Eu-PAA-*b*-PS (10)

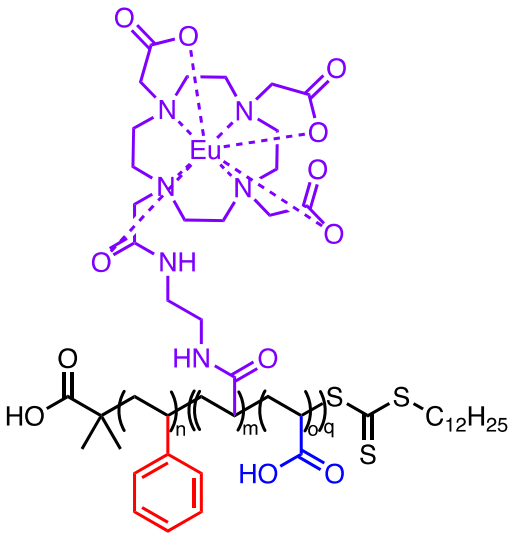

PS-*b*-PAA (**8**, 40 mg) was dispersed in H_2O (7 mL), and the reaction adjusted to pH = 8.0 using NaOH (1 M), with 1-ethyl-3-(3-dimethylaminopropyl)carbodiimide (EDC, 24 mg, 0.155 mmol) and *N*-hydroxysulfosuccinimide sodium salt (sulfo-NHS, 30 mg, 0.138 mmol) subsequently added to the reaction flask. After 30 min, 5.0 mg of **6** dissolved in of PBS (2 mL, pH = 8.0) was added with the reaction then vigorously stirred at r.t for 24 h. The solvent was removed under a stream of N_2 to afford the crude product. Afterwards, the resulting polymers were collected by washing with water three times, collecting the supernant (contains the dissolved polymer), and vacuuming off. This ensures the complete removal of any unreacted PS. Then the polymers were washed three times in MeOH to remove any unreacted reagents and left to dry under vacuum.

Paramagnetically-doped micelles: Dy-PAA-*b*-PS (11)

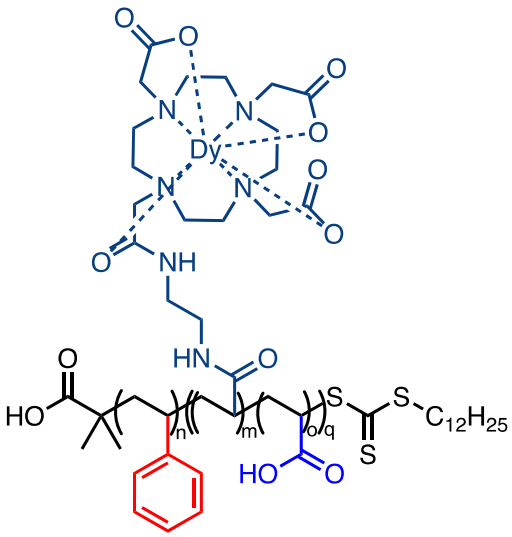

PS-*b*-PAA (**8**, 40 mg) was dispersed in H_2O (7 mL), and the reaction adjusted to pH = 8.0 using NaOH (1 M), with 1-ethyl-3-(3-dimethylaminopropyl)carbodiimide (EDC, 24 mg, 0.155 mmol) and *N*-hydroxysulfosuccinimide sodium salt (sulfo-NHS, 30 mg, 0.138 mmol) then added to the reaction flask. After 30 min, 5.0 mg of **7** dissolved in of PBS (2 mL, pH = 8.0) was added. The reaction underwent vigorous stirring at r.t for 24 h. The solvent was removed under a stream of N_2 to afford the crude product. Afterwards, the resulting polymers were collected by washing with water three times, collecting the supernant (contains the dissolved polymer), and vacuuming off. This ensures the complete removal of any unreacted PS. Then the polymers were washed twice in MeOH to remove any unreacted reagents and left to dry under vacuum.

Characterisation:

NMR spectra were recorded by dispersing the sample (c.a. 10 mg) in the desired deuterated solvent and acquired on a 2-channel Bruker AVIII 400 nanobay instrument running TOPSPIN 3 equipped with a 5 mm z-gradient broadband multinuclear probe. Dynamic Light Scattering (DLS) analysis was performed on a Malvern Zetasizer Nano with a 532 nm laser as the light source. The samples for DLS were prepared by dispersing nanoparticles (*c.a.* 1 mg mL^{-1}) in ultrapure water. The corresponding Gd^{3+} (or Dy^{3+}) concentrations were calculated and verified using inductively coupled plasma mass spectrometry (ICP-MS) analysis (Perkin Elmer NexION 2000B). The samples were prepared by hydrolysing the nanoparticles in 3 mL HNO_3 (70%) overnight. The samples were then adjusted to a final dilution of 0.3 M HNO_3 using 18.2 MΩ deionised water. The calibration curve was obtained using an external calibration analysis (a series of standards of known concentrations forming a linear plot for calibration, diluted from a 10 ppm stock standard). Gel permeation chromatography (GPC) analyses were conducted on a Shimadzu LC-20AD GPC instrument equipped with two PSS SDV 5 μm linear M columns and a refractive index (RI) detector. The samples were prepared by dissolving the polymer (*c.a.* 5 mg mL^{-1}) in 1 mL HPLC grade tetrahydrofuran (THF), and subsequently filtered through 2 μm PTFE syringe filters. This was injected into the GPC instrument using HPLC grade THF as an eluent at a flow rate of 1 mL min^{-1} (at 30 °C). RI and UV detectors were calibrated using narrow molecular weight polystyrene standards. The GPC data was analysed using a Shimadzu GPC post-run program. Samples for mass spectrometry analyses were prepared by dissolving the desired compound in a water/acetonitrile mixture (1:1 H_2O:MeCN, *c.a.* 1 mg mL^{-1}). The measurements were conducted on a Waters LCT Premier bench-top orthogonal acceleration time-of-flight LC-MS system, connected to a CTC Analytics HTS PAL Sample

Manager, Acquity PDA Detector, Acquity Column Heater/Cooler, Acquity Binary Solvent Manager. Transmission electron microscopy (TEM) images were acquired using a FEI Tecnai-T12 (USA) operated at 120 kV. The samples for TEM were prepared by depositing a drop of the aqueous colloidal suspension (*c.a.* 0.1 mg mL^{-1}) onto a copper grid. Attenuated total reflectance infrared (ATR-IR) analysis was conducted on a IRTracer-100 (Shimadzu) spectrometer.

Luminescence spectroscopy was performed using a Horiba Jobin Yvon Fluorolog-3. For sample preparation, a 20 mg mL^{-1} solution of the Eu-doped micelles was prepared in both a D_2O and H_2O buffered solution at the desired pH. For the pH/pD 4.0 measurements, an acetate buffer solution (30 mM) was used to disperse the particles, and for pH/pD 7.0 an HEPES buffered solution (30 mM) was used. An excitation wavelength of 393 nm was applied for both q value measurements.

The longitudinal relaxation times were recorded at 1.4 T using a Spinsolve Benchtop NMR (Magitrek) at room temperature. The samples were dispersed in ultrapure water at the desired Gd^{3+} concentration (dilutions of 1 mg mL^{-1}, 0.5 mg mL^{-1}, 0.25 mg mL^{-1}) with the longitudinal relaxation rate ($1/T_1$) plotted against the concentration of Gd^{3+} (mM, as determined by ICP-MS analyses). The relaxivity (mM^{-1} s^{-1}) was then obtained from the slope of the subsequent linear fit. For the transverse relaxation time measurements, the nanoparticles were dispersed in ultrapure water at the desired Dy^{3+} concentration, and the measurements performed using a Bruker AVIIIHD 500 (11.7 T). A Carr–Purcell–Meiboom–Gill (CPMG) pulse sequence was used for T_2 measurements. The relaxation rate ($1/T_2$) was plotted versus Dy^{3+} concentration (mM) and relaxivities were obtained from the slope of a subsequent linear fit.

Clinical MR imaging was performed on two scanners routinely used for both clinical research and to provide a cardiology service to NHS patients: these were Siemens 3 T Prisma and 1.5 T Avanto Fit Siemens systems, and both were sited in temperature-controlled, remotely monitored rooms. Samples were placed on the patient table and two large quality control fluid phantoms were placed nearby for coil loading purposes: all imaging was undertaken using the body coil for RF transmit, and the spine array and 18-channel coils for RF receive on each scanner. After the acquisition of localisers and an automated shimming

routine, shortened modified Look-Locker imaging (ShMOLLI) T_1 maps were acquired as described previously,[2] with a 192 x 144 acquisition matrix, 384 x 288 reconstruction matrix, 360 x 270 mm^2 FOV, 8 mm slice thickness, TE = 1.01 ms, TR = 2.06 ms, 35° readout flip angle, GRAPPA acceleration factor of 2 with 24 reference lines, 6/8 partial Fourier, inversion times 100 ms, 1100 ms, 2100 ms, 3100 ms, 4100 ms, 180 ms, 260 ms.

Results and discussion

Particle physicochemical properties

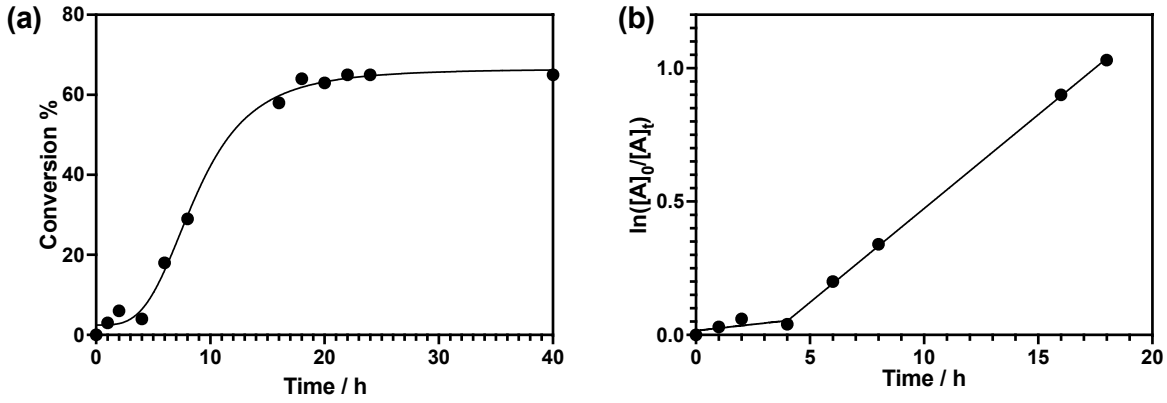

ESI 16. (a) The conversion percentage, measured by ^{1}H NMR, for PS-*b*-PAA. The maximum conversion is reached after 18 h, with a 65 % conversion. (b) Pseudo-first order kinetic plot for the RAFT polymerisation of AA.

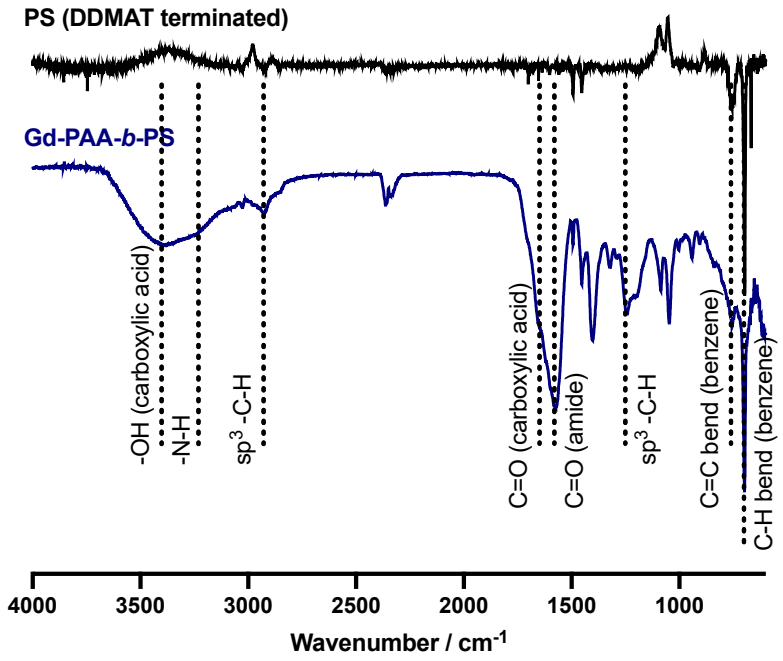

ESI 17. ATR-IR data for the polystyrene (DDMAT terminated) macroinitiator (black) and paramagnetically-doped micelles (Gd-PAA-*b*-PS, blue) with all notable peaks annotated.

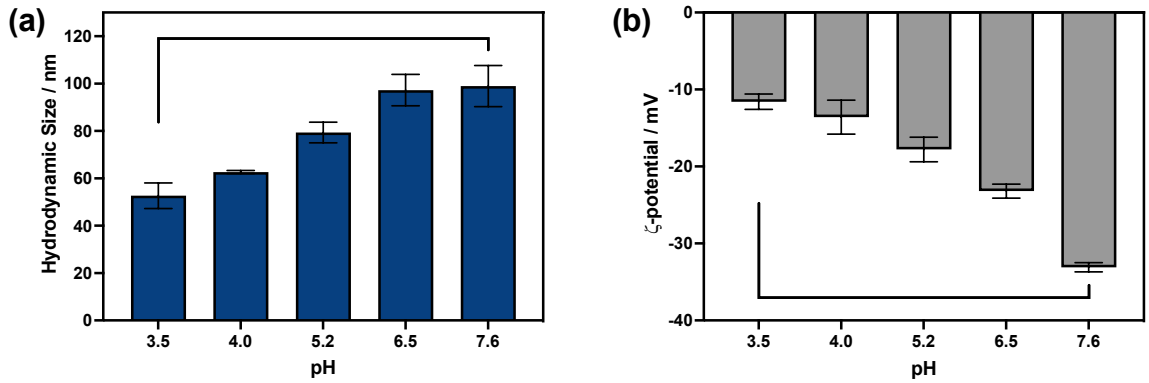

ESI 18. DLS data for a 1 mg mL^{-1} solution of the Gd-PAA-*b*-PS micelles in water for a range of different pH incubations. (a) Variations in the hydrodynamic size with pH showing clear and significant differences as the pK_a of PAA is traversed (two tail *t*-test, **, P = 0.0014). (b) Differences in ζ-potential with changes in environmental pH showing a clear and significant switch (two tail *t*-test, ****, P < 0.0001).

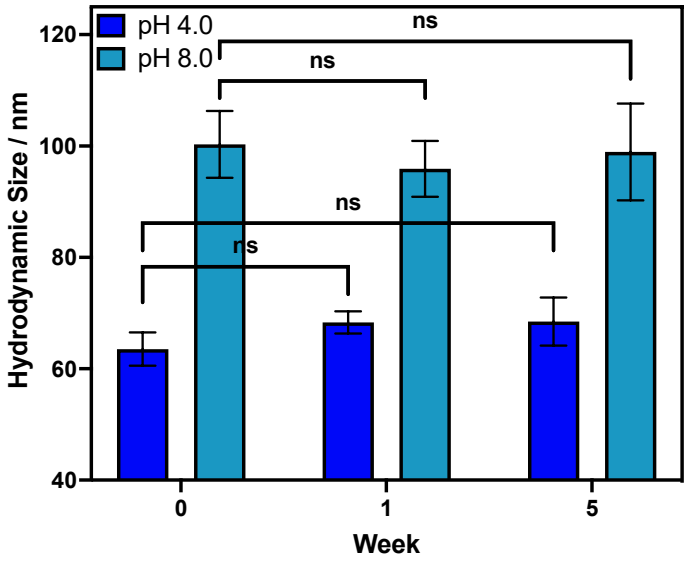

ESI 19. Stability measurements for a 1 mg mL^{-1} solution of the paramagnetically-doped micelles dispersed in water recorded over a period of 5 weeks. As can be observed, the particles exhibit high levels of colloidal stability at both pH 4.0 and 8.0, with no significant differences in hydrodynamic size as reported by DLS analyses over the measured duration (two tail *t*-test, ns, P > 0.05).

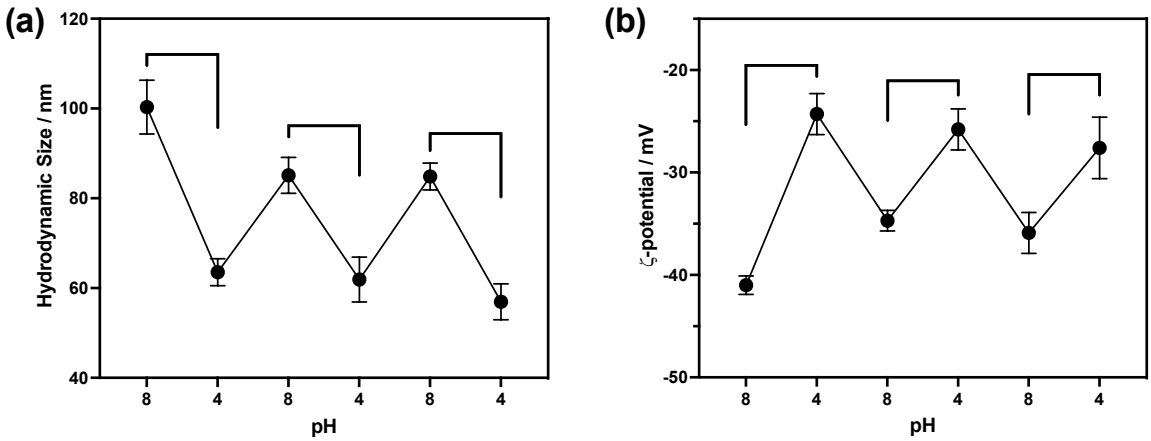

ESI 20. DLS data for a 1 mg mL^{-1} solution of the Gd-PAA-b-PS micelles incubated in water, with the pH-reversibly switched between pH 4.0 and pH 8.0 for three complete cycles. (a) Differences in hydrodynamic size with changes in pH, highlighting how reversibly switching the PAA ionisation state can have a clear and significant impact on the conformation of PAA and, by extension, the hydrodynamic size of the micelles (two tailed t-test, ***, P = 0.0006, **, P = 0.0041). (b) The reversible, and significant (two tailed t-test, ***, P = 0.0001, **, P = 0.0033, *, P = 0.0115), change in ζ-potential with repeated pH cycling.

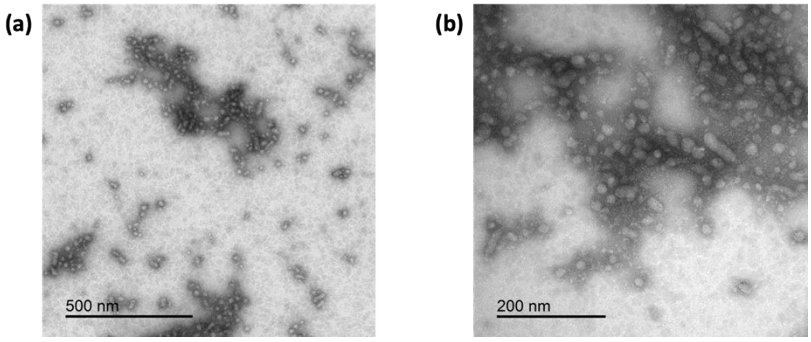

ESI 21. TEM images of the paramagnetically-doped PAA-*b*-PS micelles highlighting the formation of colloidally stable spherical micelles in solution.

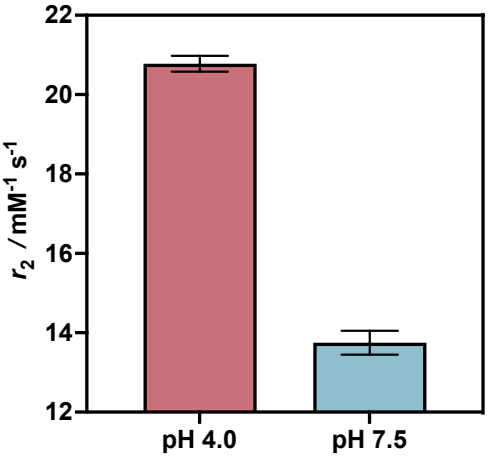

ESI 22. The transverse relaxivity values recorded at pH 4.0 and pH 7.5 for the Dy-PAA-*b*-PS micelles at 11.7 T.

q value measurements

To estimate the q value (the number of bound inner-sphere water molecules to the lanthanide centre) of the paramagnetically-modified micelles at both pH extremes, the Eu-doped analogues (Eu-PAA-*b*-PS) were synthesised. The luminescence emission spectra for Eu-PAA-*b*-PS (in acetate buffer for pH 4.0, and HEPES buffer for pH 7.0) at both pH extremes, along with the Eu-centred emission lifetime in buffered H_2O and D_2O solutions was recorded to subsequently calculate q. To achieve this, the following equation was used:[3]

$$q = 1.2\left(\frac{1}{\tau_{H_2O}} - \frac{1}{\tau_{D_2O}} - 0.25 - 0.075n\right), \quad (1)$$

where:

τ_{H_2O} is the emission lifetime of the Eu-complex measured in H_2O excited at 393 nm;

τ_{D_2O} is the emission lifetime of the Eu-complex measured in D_2O excited at 393 nm;

n is the number of oscillators ($n = 1$).

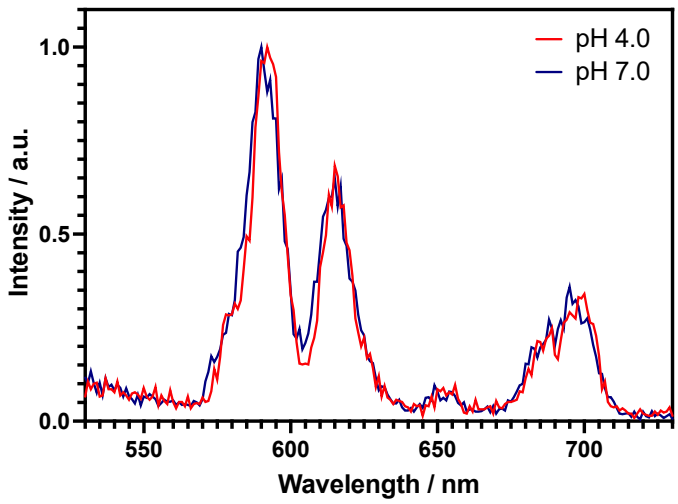

ESI 23. The emission spectra of the Eu-doped PS-*b*-PAA micelles at both pH 4.0 and pH 7.0.

Eu-PAA-*b*-PS	τ_{H_2O} / ms	τ_{D_2O} / ms	q
pH 4.0	0.59	1.95	1.0
pH 7.0	0.60	2.06	1.0

ESI 24. A table summarising the rate constants for the depopulation of the excited states of the integrated Eu-chelate within the PS-*b*-PAA micelles in H_2O and D_2O buffered solutions at pH 4.0 and 7.0. The corresponding q value at both pH is calculated using Equation 1 and included. All luminescent lifetimes are $\pm$ 10%.[3]

SBM theoretical analysis[4–6]

The observed longitudinal relaxivity value can be separated into the sum of its inner sphere (IS), second sphere (SS) and OS contributions (OS) (Eq. 1):

$$r_i = r_{i,IS} + r_{i,SS} + r_{i,OS}; \qquad i = 1, 2 \qquad (2)$$

with $i = 1, 2$ representing the longitudinal and transversal contributions respectively. The IS contribution arises from the nuclear spin residing in water molecules occupying the first coordination sphere of the paramagnetic ion and is summarised by the theory of Solomon, Bloembergen, and Morgan (SBM theory), as shown in Equation 2:

$$r_{i,IS} = \frac{q/[H_2O]}{T_{im} + \tau_m}; \qquad i = 1, 2, \qquad (3)$$

where:

q is the number of bound IS water molecules ($q = 1$);

$[H_2O]$ is the water concentration;

T_{im} is the relaxation time of the water bound to the metal ($i = 1, 2$);

τ_M is the residence lifetime of the IS water molecules ($\tau_M = 15\ ns$).

From modified SBM theory, the IS longitudinal relaxation times, T_{1m}, can be expressed as:

$$\frac{1}{T_{1,DD}}+\frac{1}{T_{1,SC}}=\frac{2}{15}\frac{C}{r_{GdH}^{6}}\left[\frac{7\tau_{c2}}{1+\omega_S^2\tau_{c2}^2}+\frac{3\tau_{c1}}{1+\omega_I^2\tau_{c1}^2}\right]+\frac{2}{3}S(S+1)\left(\frac{2\pi A}{h}\right)^2\left[\frac{\tau_e}{1+\omega_S^2\tau_{e2}^2}\right] \quad ; \quad (4)$$

where:

the constant C is given by $C=\gamma_I^2 g^2 \mu_B^2\left(\frac{\mu_0}{4\pi}\right)^2 S(S+1)$;

and:

γ_I is the proton gyromagnetic constant ($\gamma_I = 2.675\times10^{8}\,T^{-1}\,s^{-1}$);

g is the electronic g-factor ($g=2$);

S is the total electron spin of the material ion ($S=$ 7/2 for Gd^{3+});

μ_B is the Bohr magneton ($\mu_B = 9.274\times10^{-24}\,J\,T^{-1}$);

μ_0 is the vacuum permeability ($\mu_0 = 1.257\times10^{-6}\,N\,A^{-1}$);

r_{GdH} is the distance between the metal ion and proton ($r_{GdH}=0.31\,nm$);

ω_I and ω_S are the angular proton and electronic Larmor frequencies (with $\omega_S \approx 658\,\omega_I$, $\omega_I=\gamma_I B$, and B the magnetic field strength);

A is the hyperfine coupling constant (in J);

$T_{1,DD}$ and $T_{1,SC}$ are the relaxation times for the dipole-dipole and scalar relaxation mechanism between the water protons and the paramagnetic centre. The scalar contribution is often neglected and deemed to be negligible.

The dipole-dipole, τ_{c1} and τ_{c2}, and scalar, τ_e, correlation times are defined as:

$$\tau_{ci}=\left(\tau_R^{-1}+\tau_m^{-1}+T_{ie}^{-1}\right)^{-1}; \quad (5)$$

$$\tau_{ei}=\left(\tau_m^{-1}+T_{ie}^{-1}\right)^{-1}; \quad (6)$$

where $i=1,2$ is associated with T_1 or T_2 relaxation respectively.

τ_R denotes the tumbling rate of the complex;

T_{ie} are given by:

$$\frac{1}{T_{1e}} = \frac{1}{25}\Delta^2\tau_v[4S(S+1)-3]\left[\frac{1}{1+\omega_s^2\tau_v^2} + \frac{4}{1+4\omega_s^2\tau_v^2}\right]; \quad (7)$$

$$\frac{1}{T_{2e}} = \frac{1}{25}\Delta^2\tau_v[4S(S+1)-3]\left[\frac{5}{1+\omega_s^2\tau_v^2} + \frac{2}{1+4\omega_s^2\tau_v^2} + 3\right]; \quad (8)$$

where:

Δ^2 is the mean square zero field splitting (ZFS) energy ($\Delta^2 = 4.6 \times 10^{19}\, s^{-2}$);

τ_v is the correlation time for splitting ($\tau_v = 14$ ps);

Internal motion, where there are differences between the slow global motion of the supporting scaffold (e.g., inorganic nanoparticle or polymer micelle) and faster local motion due to internal flexibility, can also be modelled. This was originally reported by Lipari and Szabo and involves approximating the spectral density function as:

$$j(\omega) = \frac{F^2 3\tau_{cG1}}{(1+\omega_I^2\tau_{cG1}^2)} + \frac{(1-F^2)3\tau_{cL1}}{(1+\omega_I^2\tau_{cL1}^2)}; \quad (9)$$

where:

$$\tau_{cG1} = \left(\tau_{RG}^{-1} + \tau_M^{-1} + T_{1e}^{-1}\right)^{-1}; \quad (10)$$

$$\tau_{cL1} = \left(\tau_{cG1}^{-1} + \tau_{RL}^{-1}\right)^{-1}; \quad (11)$$

and:

F denotes an order parameter that takes a value between 0 and 1;

τ_{RG} is the global correlation time;

τ_{RL} is the local correlation time;

τ_{cL1} the local correlation time which accounts for fast local motion ($^{1}/_{\tau_{cL1}} = {}^{1}/_{\tau_{cG1}} + {}^{1}/_{\tau_{RL}}$).

Depending on the value of F^2 the motion is either governed by the global relaxation time ($F^2 = 1$) or the fast local motion ($F^2 = 0$).

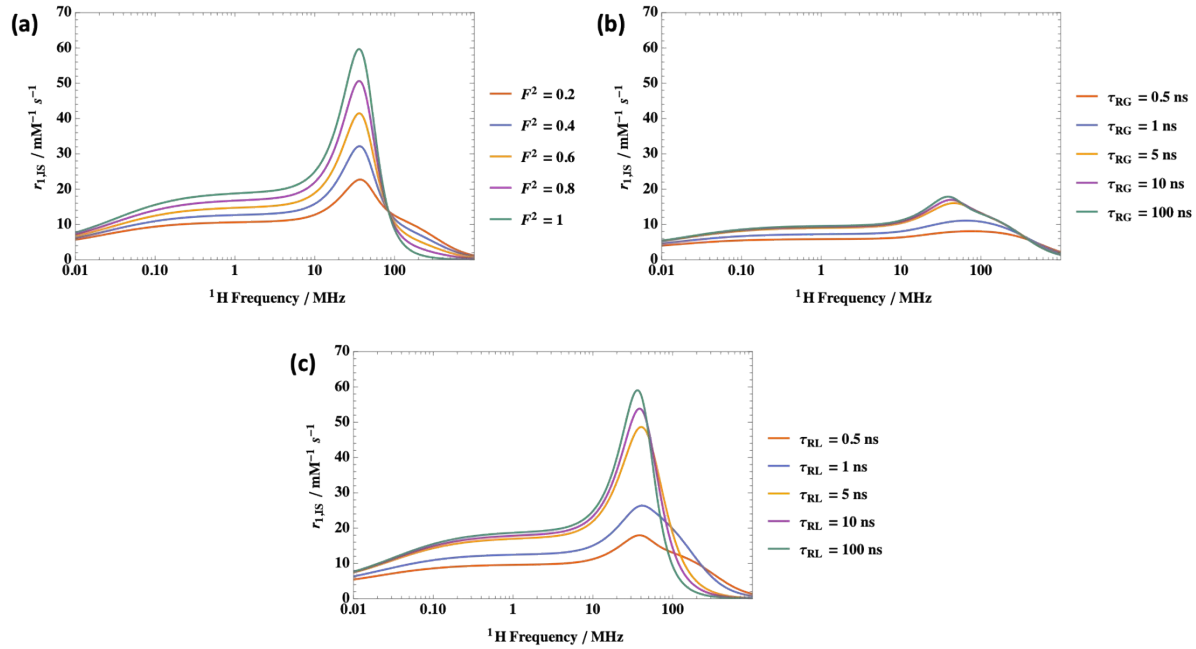

ESI 25. Theoretical SBM plots highlighting the importance of optimising over . (a) Lipari-Szabo modified SBM plot to highlight how differences in the contributions of and , as defined by an order parameter , affects the inner-sphere relaxivity of the micelle (b) This plot demonstrates that increases in are small when internal motion is fast, regardless of the extent of elongation of (= 50 ns). (c) A plot emphasising the contribution of to , and its importance over the global rotational correlation time (= 50 ns).

MRI analysis

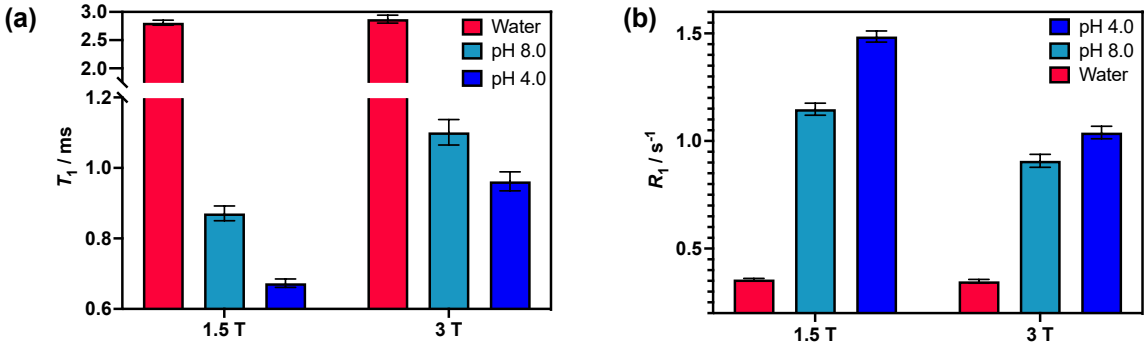

ESI 26. The MRI derived (a) relaxation times and (b) relaxation rate for a 1 mg mL^{-1} solution of the Gd-PAA-*b*-PS micelles incubated in water at both pH 4.0 and 8.0 (pure water is included as a reference).

T_1

References:

1 W. S. Perry, S. J. A. Pope, C. Allain, B. J. Coe, A. M. Kenwright and S. Faulkner, *Dalt. Trans.*, 2010, **39**, 10974–10983.

2 S. K. Piechnik, V. M. Ferreira, E. Dall'Armellina, L. E. Cochlin, A. Greiser, S. Neubauer and M. D. Robson, *J. Cardiovasc. Magn. Reson.*, 2010, **12**, 1–11.

3 A. Beeby, I. M. Clarkson, R. S. Dickins, S. Faulkner, D. Parker, L. Royle, A. S. De Sousa, J. A. G. Williams and M. Woods, *J. Chem. Soc. Perkin Trans. 2*, 1999, 493–503.

4 P. Caravan, C. T. Farrar, L. Frullano and R. Uppal, *Contrast Media Mol. Imaging*, 2009, **4**, 89–100.

5 G. Lipari and A. Szabo, *J. Am. Chem. Soc.*, 1982, **104**, 4559–4570.

6 J. S. Ananta, B. Godin, R. Sethi, L. Moriggi, X. Liu, R. E. Serda, R. Krishnamurthy, R. Muthupillai, R. D. Bolskar, L. Helm, M. Ferrari, L. J. Wilson and P. Decuzzi, *Nat. Nanotechnol.*, 2010, **5**, 815–821.